Ultrafast Carbon-Carbon Single-Bond Rotational Isomerization in Room-Temperature Solution

Junrong Zheng, Kyungwon Kwak, Jia Xie, M. D. Fayer

Generally, rotational isomerization about the carbon-carbon single bond in simple ethane derivatives in room-temperature solution under thermal equilibrium conditions has been too fast to measure. We achieved this goal using two-dimensional infrared vibrational echo spectroscopy to observe isomerization between the gauche and trans conformations of an ethane derivative, 1-fluoro-2-isocyanato-ethane (**1**), in a CCl_4 solution at room temperature. The isomerization time constant is 43 picoseconds (ps, 10^{-12} s). Based on this value and on density functional theory calculations of the barrier heights of **1**, *n*-butane, and ethane, the time constants for *n*-butane and ethane internal rotation under the same conditions are ~40 and ~12 ps, respectively.

Many molecules can undergo rotational isomerization around one or more of their chemical bonds. During the course of isomerization, a molecule exchanges between relatively stable conformations by passing through unstable configurations. Rotational isomerization is a major factor in the dynamics, reactivity, and biological activity of a multiplicity of molecular structures. Ethane and its derivatives are textbook examples of molecules that undergo this type of isomerization. (*1*) In ethane, as one of the two methyl groups rotates 360° around the central carbon-carbon single bond, it will alternate three times between an unstable eclipsed conformation and the

Department of Chemistry, Stanford University, Stanford, CA 94305, USA.

preferred staggered conformation. The transition from one staggered state to another leaves ethane structurally identical. Therefore, the result of ethane isomerization cannot be observed through a change in chemical structure. In a 1,2-disubstituted ethane derivative, the molecule can undergo a similar isomerization. However, a 1,2-disubstituted ethane has two distinct staggered conformations, gauche and trans (anti), and two eclipsed conformations, anticlinal and synperiplanar, because of the distinguishing characteristics of the relative positions of the two substituents (Fig. 1A) (*1*). The isomerization is frequently referred to as "hindered internal rotation" (*2*). It has been the subject of intense theoretical and experimental study since Bischoff found 100 years ago that rotation about the C-C single bond in ethane is not completely free. (*2*)

The trans-gauche isomerization of 1,2-disubstituted ethane derivatives, such as *n*-butane, is one of the simplest cases of a first-order chemical reaction. This type of isomerization has served as a basic model for modern chemical reaction kinetic theory and molecular dynamics (MD) simulation studies in condensed phases of matter (*3*–*8*). In spite of extensive theoretical investigation, no corresponding kinetic experiments have been performed to test the results, partially because of the low rotational energy barrier of the *n*-butane (~3.4 kcal/mol) and of other simple 1,2-disubstituted ethane derivatives (*9*). According to theoretical studies (*3*–*8*), the isomerization time scale (1/*k*, where *k* is the rate constant) is 10 to 100 ps at room temperature in liquids.

The room-temperature time scale is much shorter than the microsecond and longer–time scale measurements that can be made with dynamic nuclear magnetic resonance (DNMR) spectroscopy, a widely used method for studying slow temperature-dependent isomerization kinetics (*10*). The picosecond kinetics at room temperature cannot be deduced from microsecond or millisecond dynamics at low temperature because the rate constant is not a simple function of temperature over a wide temperature range (*11*). Thus, DNMR does not afford accurate estimates of isomerization rates at room temperature for molecules with small barriers, such as ethane, that rotate in tens of picoseconds. Other methods to study fast isomerization dynamics under thermal equilibrium, such as linear infrared (IR) and Raman line shape analysis (*12*, *13*), are hampered by multiple contributing factors apart from isomerization (*14*–*16*).

Two-dimensional (2D) IR vibrational echo chemical exchange spectroscopy has recently proven useful for studying fast dynamical processes under thermal equilibrium conditions (*17*–*19*). We applied this method to study the ultrafast trans-gauche isomerization dynamics of a simple 1,2-disubstituted ethane derivative, 1-fluoro-2-isocyanato-ethane (**1**), at room temperature in liquid solution. The experiments were performed by observing the time dependence of the 2D spectrum of the isocyanate group's antisymmetric stretching mode.

Details of the methodology of 2D IR vibrational echo spectroscopy have been described previously (*20*). Very briefly, in a 2D IR vibrational echo experiment, three ultrashort IR pulses tuned to the frequency of the vibrational modes of interest are crossed in the sample. Because the pulses are very short, they have a broad bandwidth that makes it possible to simultaneously excite a number of vibrational modes. The first laser pulse "labels" the initial structures of the species in the sample by setting their initial frequency, ω_τ. The second pulse ends the first time period τ and starts clocking the reaction time period T_w during which the labeled species undergo isomerization and other population dynamics changes such as vibrational relaxation to the ground state and orientational relaxation of the entire molecule. The third pulse ends the population dynamics period of length T_w and begins a third period of length $\leq\tau$, which ends with the emission of the vibrational echo pulse of frequency ω_m. The vibrational echo signal reads out information about the final structures of all labeled species by their frequency ω_m.

There are two types of time periods in the experiment. The times between pulses 1 and 2 and between pulse 3 and the echo pulse are called coherence periods. During these periods, the vibrations are in coherent superpositions of two vibrational states. Fast vibrational oscillator frequency fluctuations induced by fast structural fluctuation of the system cause dynamic dephasing, which is one contribution to the line shapes in the conventional 1D absorption spectrum. During the period T_w between pulses 2 and 3, called the population period, a vibration is in a distinct eigenstate rather than a superposition state. Slow structural fluctuations of the system, termed spectral diffusion, contribute to the 2D line shapes. Other processes during the population period, particularly chemical exchange, also produce changes in the 2D spectrum. Chemical exchange occurs when two species in equilibrium interconvert without changing the overall number of either species. Isomerization back and forth between gauche and trans conformations of **1** is a type of chemical exchange. In other contexts, it has been demonstrated that chemical exchange causes new peaks to grow in as T_w is increased (*17*–*19*). In our experiments, the growth of off-diagonal peaks in the 2D vibrational echo spectrum of **1** with increasing T_w was used to extract the gauche-trans isomerization rate.

The calculated structures and potential energy of **1** as it undergoes rotational isomerization about the central carbon-carbon single bond (Fig. 1, A and B) were obtained using density functional theory (DFT) (*21*) at the B3LYP level and 6-31+G(d,p) basis set for isolated molecules. The energy values were corrected for the zero point energy. The gauche-trans isomerization has two possible transition states: the anticlinal conformer, where the F atom is eclipsed by the H atom; and the synperiplanar conformer, where the F atom is eclipsed by the N atom. Calculations show that the anticlinal conformer is the transition state because it has a much lower energy (3.3 kcal/mol) than the synperiplanar conformer (>7 cal/mol). From the cal-

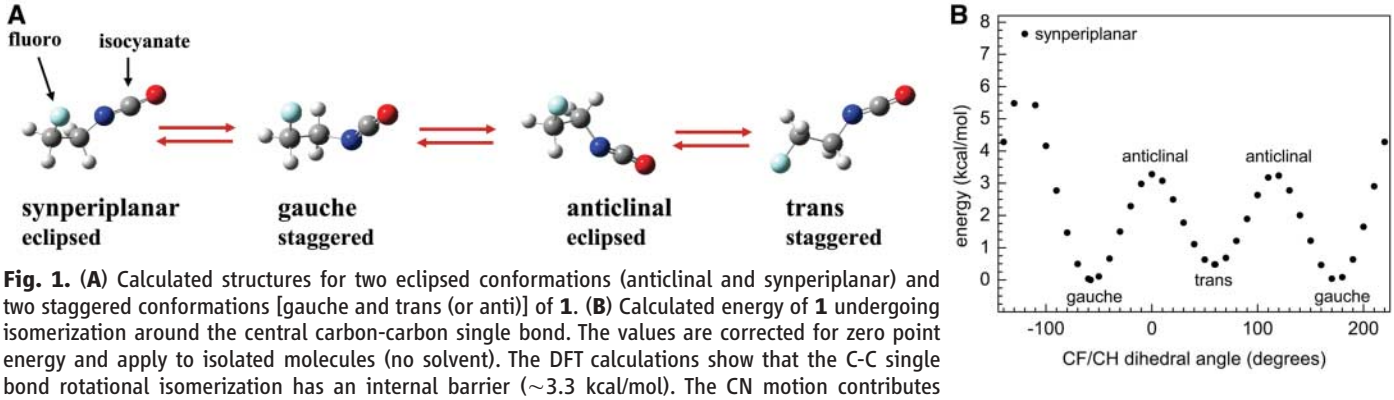

Fig. 1. (**A**) Calculated structures for two eclipsed conformations (anticlinal and synperiplanar) and two staggered conformations [gauche and trans (or anti)] of **1**. (**B**) Calculated energy of **1** undergoing isomerization around the central carbon-carbon single bond. The values are corrected for zero point energy and apply to isolated molecules (no solvent). The DFT calculations show that the C-C single bond rotational isomerization has an internal barrier (~3.3 kcal/mol). The CN motion contributes only slightly to the energy of the configurational change. Thus, the exchange rate between the gauche and trans conformers is essentially the C-C single-bond rotational isomerization rate. The calculations also demonstrate that during exchange between the gauche and trans conformers, the molecule passes through a transition state, the eclipsed conformation (anticlinal), that is similar to the one calculated for ethane isomerization.

culations for the isolated molecule (no solvent), the gauche conformer is about 0.5 kcal/mol more stable than the trans conformer.

The gauche and trans conformers have different geometries and intramolecular interactions, resulting in different vibrational frequencies for the antisymmetric stretching mode of the isocyanate group (NCO) and different dipole moments. Calculations show that the trans conformer has an NCO stretching frequency ~15 cm^{-1} higher than the gauche conformer. In the Fourier transform infrared (FTIR) spectroscopy spectrum of the NCO antisymmetric stretching mode of **1** in CCl_4 at room temperature, there are two peaks of similar intensity (Fig. 2). Based on the calculations, the peak at 2280 cm^{-1} is assigned to the trans conformer and the one at 2265 cm^{-1} to the gauche. The population ratio of trans/gauche (the equilibrium constant) is ~1:1, obtained by analyzing both the 1D and 2D IR data (*19*) (fig. S1). The population ratio was experimentally determined to be temperature- and solvent polarity–dependent, demonstrating that two equilibrated species exist in the system. However, the linear IR spectrum cannot provide information about the isomerization kinetics.

Figure 3A displays six T_w-dependent 2D IR spectra of **1** in a CCl_4 solution at room temperature. The 0-fs panel corresponds to the shortest T_w, at which negligible isomerization has occurred. As discussed in detail previously (*17*), when no isomerization has occurred, the initial and final structures of each labeled species in the sample are unchanged. Therefore, the ω_τ and ω_m values of each peak are identical, and the peaks appear only on the diagonal. The two peaks representing the gauche (ω_m = 2265 cm^{-1}) and trans (ω_m = 2280 cm^{-1}) conformers are clearly visible on the diagonal. After a long reaction period (T_w = 25 ps), isomerization has proceeded to a substantial degree. The obvious change is the additional peak that has appeared at the upper left (ω_τ = 2265 cm^{-1} and ω_m = 2280 cm^{-1}). This peak arises from gauche-to-trans isomerization. There is a corresponding peak to the lower right that is generated by trans-to-gauche isomerization, but it is somewhat negated by a negative-trending peak produced by population relaxation (*22*) between the antisymmetric isocyanate mode and another mode (fig. S1). The negative-trending (blue) peaks due to population relaxation are discussed further below and in the supporting material. They are included in the detailed fitting of the data. The diagonal peaks arise from molecules with the same initial and final structures; that is, molecules that either did not undergo isomerization during the time period T_w or else underwent multiple isomerization cycles that left them in their initial conformation at the end of the T_w period. The growth of the off-diagonal peaks with increasing T_w permits determination of the isomerization rate (chemical exchange rate), although it is necessary to analyze the growth and decay of all the peaks for accuracy (*19*).

During the T_w period, other factors besides chemical exchange also influence the 2D spectrum. These phenomena include spectral diffusion, orientational relaxation, and vibrational relaxation (*17*). Spectral diffusion changes the shape of each peak, and the orientational and vibrational relaxations cause all peaks to decrease in amplitude. Only chemical exchange produces growing off-diagonal positive-trending (red) peaks for the two distinct species. There is an additional vibrational relaxation pathway, distinct from the regular vibrational lifetime decay, that stems from the coupling of the NCO antisymmetric stretch of both conformers to a vibrational mode of unassigned nature at ~2230 cm^{-1} (fig. S1). The coupling induces fast back-and-forth population equilibration between the unassigned mode and the NCO antisymmetric stretch [equilibration time constants are 0.9 ps for the trans conformation and 1.9 ps for the gauche conformation (fig. S2)]. The equilibration via vibrational relaxation also produces additional negative (blue) peaks (*22*) just below each positive (red) peak. As shown at the very bottom of each panel in Fig. 3A, two blue peaks at low frequency along ω_m grow in with T_w. The off-diagonal red peak at ω_τ = 2280 cm^{-1} and ω_m = 2265 cm^{-1} (lower right) is smaller than the upper left off-diagonal peak because of canceling overlap with a negative vibrational relaxation blue peak at approximately ω_τ = 2280 cm^{-1} and ω_m = 2270 cm^{-1}.

Assignment of the growing positive (red) off-diagonal peaks to isomerization, with the one at the lower right offset by an overlapping negative-trending (blue) peak, can be confirmed by examining 1-bromo-2-isocyanato-ethane. The bromo group is so large that it generates substantial steric hindrance in the eclipsed form

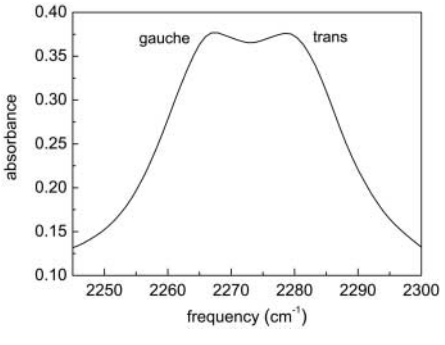

Fig. 2. FTIR spectrum of **1** in a CCl_4 solution at room temperature. Calculations assign the peak at ~2280 cm^{-1} to the trans conformer and the peak at ~2265 cm^{-1} to the gauche conformer.

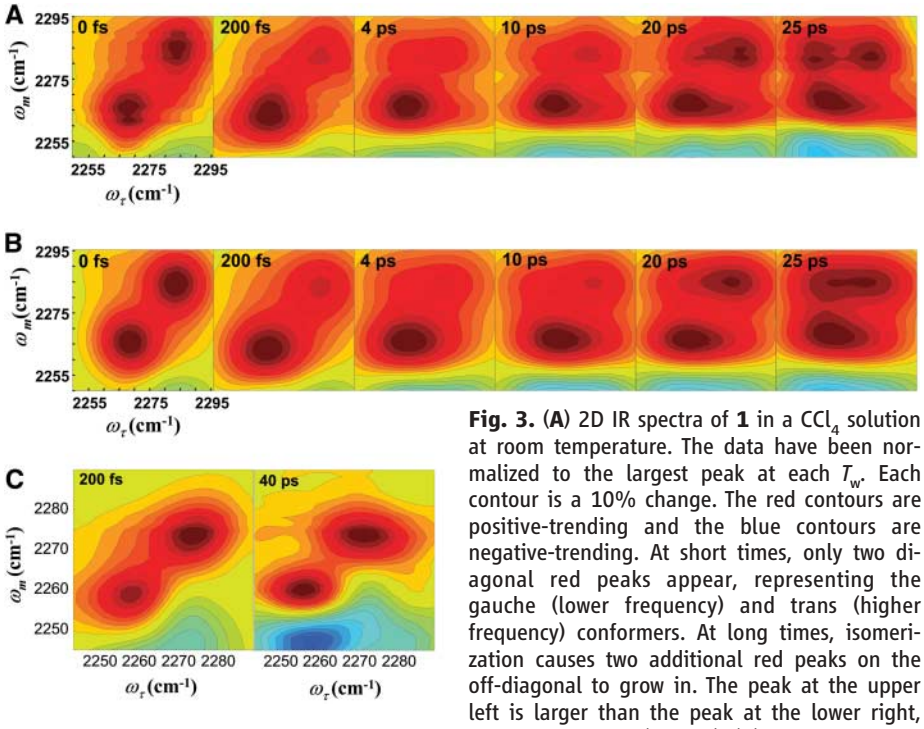

Fig. 3. (**A**) 2D IR spectra of **1** in a CCl_4 solution at room temperature. The data have been normalized to the largest peak at each T_w. Each contour is a 10% change. The red contours are positive-trending and the blue contours are negative-trending. At short times, only two diagonal red peaks appear, representing the gauche (lower frequency) and trans (higher frequency) conformers. At long times, isomerization causes two additional red peaks on the off-diagonal to grow in. The peak at the upper left is larger than the peak at the lower right, because the lower right peak overlaps with a negative-trending peak (Fig. 3C). (**B**) Calculated 2D IR spectra using the model and procedures discussed in the text and in the supporting online material. The agreement between the experiments and the calculated spectra is very good. (**C**) 2D IR spectra of 1-bromo-2-isocyanato-ethane in a CCl_4 solution at room temperature. The bulky bromo group prevents isomerization from occurring past T_w = 40 ps. All other aspects of the system are the same as for **1**. The results show that the positive-trending (red) off-diagonal peaks do not grow in without isomerization. The negative trending peak to the lower right that interferes with the positive-trending isomerization peak in Fig. 3A is apparent.

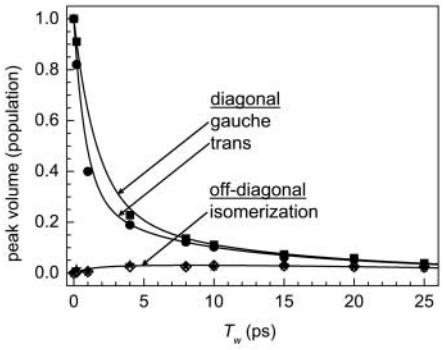

Fig. 4. Data (points) and calculated curves for the 2D spectra, some of which are shown in Fig. 3A. The points are the T_w-dependent peak volumes for the two diagonal and two off-diagonal peaks. The solid curves are all calculated with a single adjustable parameter, the isomerization time constant. The agreement is very good and yields an isomerization time constant of 43 ps. Input parameters of the model, all measured experimentally, are the equilibrium constant $K_{eq} = 1$; orientational relaxation time constants $\tau_T = 3.2$ ps (T, trans) and $\tau_G = 3.4$ ps (G, gauche); and vibrational relaxation time constants $T_T^{fast} = 0.91$ ps with normalized amplitude 0.63, $T_T^{slow} = 18.8$ ps with normalized amplitude 0.37, $T_G^{fast} = 1.95$ ps with normalized amplitude 0.6, and $T_G^{slow} = 18.4$ ps with normalized amplitude 0.4.

and greatly raises the barrier for isomerization. On the time scale of interest here, isomerization does not occur. All other aspects of the system are the same, including the vibrational population equilibration with the unassigned peak. Figure 3C displays 2D IR spectra for a 1-bromo-2-isocyanato-ethane/CCl_4 solution at room temperature at short and long T_w. At 40 ps, no positive-trending (red) off-diagonal peaks have appeared, indicating that the isomerization time constant is much greater than 100 ps. In the absence of the positive-trending off-diagonal isomerization peaks, the negative-trending population equilibration peak that interferes with the lower right isomerization peak in the spectrum of **1** is clearly visible.

To quantitatively model the 2D spectra and extract the kinetic parameters from the 2D IR data, a modified version of the kinetic model described previously was used (*17*, *19*). The trans and gauche conformers undergo isomerization, which results in chemical exchange in the spectra. The amplitudes of the signals for each species decay because of orientational relaxation, fast vibrational relaxation (vibrational equilibration), and slower vibrational lifetime decay to the ground state (fig. S3). The kinetic model requires as inputs the orientational relaxation times and the fast (equilibration) and slow (decay to the ground state) vibrational relaxation times to model the data and obtain the isomerization rate constant. The orientational relaxation and vibrational relaxation time constants were measured with polarization-selective pump-probe experiments (*19*, *23*) (fig. S2). The equilibrium constant ($K_{eq} = 1$) and the vibrational transition dipole moment ratio (~1) were obtained by analyzing both the 1D IR spectrum and the 2D IR spectrum at $T_w = 0$ fs (fig. S1). (*19*) The time-dependent populations are provided by the peak volumes of the four red peaks in 2D IR spectra scaled with the transition dipole moment ratio. Therefore, only one unknown parameter, the isomerization rate constant $k_{TG} = k_{GT}$, was used in the fitting. The trans-to-gauche (TG) and gauche-to-trans (GT) rate constants are taken to be equal within experimental error because the equilibrium constant is 1.

Figure 3B shows calculated 2D spectra using the known input parameters and the results of fitting k_{TG}. Both the measured and calculated spectra are normalized by scaling to make the largest peak at each time equal to unity. Given the complexity of the system, the model calculations do a very good job of reproducing the time-dependent data. Of particular importance is the growth of the off-diagonal red peaks and the negative-trending peaks at the bottom of each panel. The data are well fit using the isomerization rate constant as the only adjustable parameter (Fig. 4). The off-diagonal peaks grow in at the same rate, consistent with $k_{TG} = k_{GT}$ within experimental error. The fits yield $1/k_{TG} = 1/k_{GT} = 43 \pm 10$ ps. The error bars arise from the uncertainty in the parameters that go into the calculations.

Based on the experimental results for the 1-fluoro-2-isocyanato-ethane, it is possible to calculate approximately the gauche-trans isomerization rate of *n*-butane and the rotational isomerization rate of ethane under the same conditions used in this study (CCl_4 solution at room temperature, 297 K). We have analyzed *n*-butane because there is a large number of theoretical calculations for the isomerization of this molecule (*5*–*8*). Transition state theory (*11*) was employed, with the assumption that the prefactors for all of the systems are the same. This assumption is reasonable because the transition states and the barrier heights are quite similar for the three systems. We performed DFT calculations on all the systems using the same method [the B3LYP level and 6-31+ G(d,p) basis set] to obtain the barrier heights. With the zero point energy correction, the trans-to-gauche isomerization of *n*-butane has a barrier of 3.3 kcal/mol. The barrier for ethane is calculated to be 2.5 kcal/mol. This value differs from the 2.9 kcal/mol (*24*, *25*) that has been obtained using more extensive electronic structure calculations. However, here we will employ the 2.5 kcal/mol value for comparison with the 3.3 kcal/mol obtained for **1**. By calculating the two barriers with the same method, there should be some cancellation of errors.

Using the calculated barriers for **1** and for *n*-butane and the assumption that the prefactors are the same, we obtain a ~40 ps time constant for the *n*-butane trans-to-gauche isomerization time constant ($1/k_{TG}$). Twenty-six years ago, Rosenberg, Berne, and Chandler reported a 43-ps time constant for this process (in CCl_4 at 300 K) from MD simulations. (*6*) Other MD simulations gave isomerization rates in liquid *n*-butane at slightly lower temperatures: 52 ps (292 K) (*7*), 57 ps (292 K) (*5*), 50 ps (273 K) (*5*), and 61 ps (<292 K) (*8*). All of these values are reasonably close to the value obtained here based on the experimental measurements of **1**. In the same manner, the isomerization time constant for ethane is found to be ~12 ps. This value can be improved by better electronic structure calculations on **1** and calculations for both **1** and ethane that include the CCl_4 in determining the barriers.

This 2D IR vibrational echo technique should be generally applicable to the study of fast isomerizations, most of which give rise to conformers with necessarily distinct vibrational spectra. For the method to be useful, the isomerization time constant must fall into a time window determined by experimental considerations. The lower time limit of the method is determined by the laser pulse duration, which can be <50 fs and therefore is not a serious restriction. The upper time limit is determined by the vibrational lifetime of the mode used to probe the isomerization. In practice, the isomerization time constant should be less than three times the vibrational lifetime. Some modes, such as the CO stretches of metal carbonyl compounds, can have lifetimes of hundreds of picoseconds. Within the experimental limitations, the method used here should be useful for addressing a variety of important problems.

References and Notes

1. J. March, *Advanced Organic Chemistry* (Wiley, New York, 3rd ed., 1985).
2. W. J. Orville-Thomas, *Internal Rotation in Molecules* (Wiley, New York, 1974).
3. D. Chandler, *J. Chem. Phys.* **68**, 2959 (1978).
4. T. A. Weber, *J. Chem. Phys.* **69**, 2347 (1978).
5. D. Brown, J. H. R. Clarke, *J. Chem. Phys.* **92**, 3062 (1990).
6. R. O. Rosenberg, B. J. Berne, D. Chandler, *Chem. Phys. Lett.* **75**, 162 (1980).
7. R. Edberg, D. J. Evans, G. P. Morris, *J. Chem. Phys.* **87**, 5700 (1987).
8. J. Ramirez, M. Laso, *J. Chem. Phys.* **115**, 7285 (2001).
9. A. Streitwieser, R. W. Taft, *Progress in Physical Organic Chemistry* (Wiley, New York, 1968), vol. 6.
10. L. M. Jackman, F. A. Cotton, *Dynamic Nuclear Magnetic Resonance Spectroscopy* (Academic Press, New York, 1975).
11. I. N. Levine, *Physical Chemistry* (McGraw-Hill, New York, 1978).
12. B. Cohen, S. Weiss, *J. Phys. Chem.* **87**, 3606 (1983).
13. J. J. Turner *et al.*, *J. Am. Chem. Soc.* **113**, 8347 (1991).
14. R. A. MacPhail, H. L. Strauss, *J. Chem. Phys.* **82**, 1156 (1985).
15. H. L. Strauss, *J. Am. Chem. Soc.* **114**, 905 (1992).
16. N. E. Levinger *et al.*, *J. Chem. Phys.* **118**, 1312 (2003).
17. J. Zheng *et al.*, *Science* **309**, 1338 (2005).
18. Y. S. Kim, R. M. Hochstrasser, *Proc. Natl. Acad. Sci. U.S.A.* **102**, 11185 (2005).
19. J. Zheng, K. Kwak, X. Chen, J. B. Asbury, M. D. Fayer, *J. Am. Chem. Soc.* **128**, 2977 (2006).
20. J. B. Asbury, T. Steinel, M. D. Fayer, *J. Lumin.* **107**, 271 (2004).

21. R. G. Parr, W. Yang, *Density Functional Theory of Atoms and Molecules* (Oxford Univ. Press, New York, 1989).
22. M. Khalil, N. Demirdoven, A. Tokmakoff, *J. Chem. Phys.* **121**, 362 (2004).
23. H.-S. Tan, I. R. Piletic, M. D. Fayer, *J. Opt. Soc. Am. B* **22**, 2009 (2005).
24. V. Pophristic, L. Goodman, *Nature* **411**, 565 (2001).
25. F. M. Bickelhaupt, E. J. Baerends, *Angew. Chem. Int. Ed.* **42**, 4183 (2003).
26. We thank X. Chen and J. I. Brauman for insightful discussions. This work was supported by grants from the Air Force Office of Scientific Research (F49620-01-1-0018) and NSF's Division of Materials Research (DMR-0332692).

Supporting Online Material

www.sciencemag.org/cgi/content/full/313/5795/1951/DC1
Figs. S1 to S3
References

6 July 2006; accepted 21 August 2006
10.1126/science.1132178